Na CHANNEL KINETICS DURING THE SPONTANEOUS HEART BEAT IN EMBRYONIC CHICK VENTRICLE CELLS

MICHELE MAZZANTI AND LOUIS J. DEFELICE
Department of Anatomy and Cell Biology, Emory University, Atlanta, Georgia 30322

ABSTRACT Using cell-attached and whole-cell recording techniques simultaneously allows the measurement of Na currents during action potentials in beating heart cells. In 7-d chick ventricle, the dynamic reversal potential for Na is 30 mV, which is 20 mV less than the reversal potential in nonbeating cells. This result implies that the spontaneous activity of heart cells raises the Na concentration at the internal face of the membrane to nearly 40 mM. Fitting the Na action currents to the Hodgkin and Huxley equations shows that patches may contain from 50 to 700 Na channels, with an average density of 23 ± 21 per μm^2. Only ~2% of the available Na channels are open at the peak of the Na action current. This low probability is a consequence of the channels' continual inactivation during the diastolic depolarization phase.

INTRODUCTION

The seminal work of Hodgkin and Huxley (1952) has been the major influence on virtually all research into the nature of Na channels. In fact, departures from their original protocols have been surprisingly few. Since Hodgkin and Huxley, the development of the patch-clamp technique and the measurement of currents through individual channels have further advanced Na channel research. Although the patch method created the possibility of studying Na channels without disturbing their surroundings, most research has continued to isolate the channel from the broader context of its native state. Moreover, the traditional voltage-clamp experiments expose the channels to abrupt changes in voltage they ordinarily never experience.

In cardiac tissue, the basis for virtually all models of the Na current and reconstructions of action potentials are two-microelectrode, voltage-clamp experiments on multicellular preparations (McAllister et al., 1975, Purkinje fibers; Beeler and Reuter, 1977, adult ventricle; Ebihara and Johnson, 1980, embryonic chick ventricle; DiFrancesco and Noble, 1985, Purkinje fibers; and Shrier and Clay, 1986, embryonic chick ventricle). Na currents from individual cells resemble those from whole tissue (Lee et al., 1979; Brown et al., 1981; Lee et al., 1981; Bodewei et al., 1982; Cachelin et al., 1982; Kunze et al., 1985; and Fujii et al., 1986). Most representations of the Na current follow the Hodgkin and Huxley (1952) equations for nerve axon. The principal differences lie in the exact formulation of the rate constants. For Na, these constants are usually smaller in heart than in nerve, with the result that kinetics are slower and inactivation is stronger in the cardiac Na channel. In addition, $\bar{g}_{Na}$ is much smaller, indicating a lower density of Na channels in heart than in nerve.

Using the cell-attached, patch electrode technique on a beating cell, the present study provides a fresh view of the Na channel during its natural dynamic condition, which includes not only membrane potential but also chemical environment. By assuming models of the Na channel in which kinetics are purely voltage dependent, and by expecting these kinetics to translate from the rather different circumstances of step-protocol experiments to the condition of beating, the present experimental results reassess the basic premise of virtually all models of the channel's action. The data also provide the contribution of Na to the cardiac action potential directly and without recourse to any particular model.

MATERIALS AND METHODS

Embryonic ventricle cells were prepared by enzymatic digestion of 7-d chick embryo hearts, following the procedure of DeHaan (1967). After 12–24 h in tissue culture medium, and immediately preceding the experiments, we washed the cells with bath solution at room temperature. The composition of the bath (in millimolars) was: 130 Na, 1.3 K, 1.5 Ca, 0.5 Mg, 1 SO4, 133.5 Cl, 5 dextrose, 10 Hepes, pH 7.35; the cell-attached electrode contained the same solution. The whole-cell electrode contained an intracellular-like solution consisting of 140 K, 0.1 Ca, 2 Mg, 122.1 Cl, 1.1 EGTA, 10 Hepes, pH 7.4.

The patch electrodes were made from borosilicate glass (Corning 7052; Corning Glass Works, Corning, NY) using a programmable puller (Sachs-Flaming, PC-84, Sutter Instrument). After the electrodes were coated with Sylgard (Dow Corning Corp. Midland, MI) and the tip was fire polished to 1–3 mm diameter, the electrodes had resistances of 4–10 mMΩ. The method of dual whole-cell and patch recordings follows Fischmeister et al. (1984). The current and voltage electrodes were usually ~5–20 μm apart (see Fig. 1). By breaking the patch in the current electrode and switching to current clamp, we could show that both electrodes measured the same voltage, thus, the single cells or small clusters of cells were space clamped.

List EPC5 and EPC7 amplifiers measured the voltage and current. A

Dr. Mazzanti's permanent address is Fisiologia e Biochemica Generale, Via Celoria, 26, 20133 Milan, Italy.

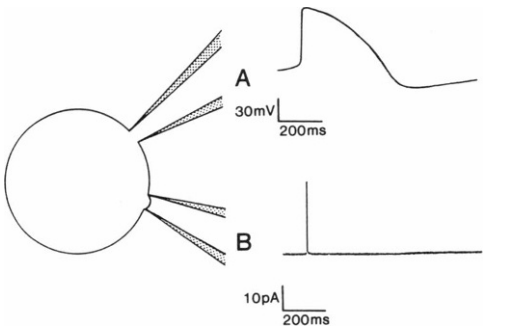

FIGURE 1 Experimental arrangement. (*A*) An electrode in the whole-cell, current-clamp configuration records an action potential during one beat of a cardiac myocyte. (*B*) At the same time, an electrode in the cell-attached, voltage-clamp mode measures the current through a patch. This patch contains so few channels that none open during this particular beat.

VCR (Panasonic Co., Secaucus, NJ) stored the data, which we analyzed on an oscilloscope (model 4094; Nicolet Instrument Corp., Madison, WI) and an IBM-AT (IBM Instruments, Danbury, CT). To compare the data with theoretical models, we simulated Na action currents from ensembles of channels obeying specific kinetic schemes, such as the HH m^3h model (DeFelice et al., 1985).

RESULTS

Measurement of the Patch Capacitance

Fig. 1 illustrates the simultaneous measurement of patch current and cell potential. The patch contained no apparent ionic currents. Assuming the transient in Fig. 1 *B* is purely capacitive:

$$i_c(t) = c(\mathrm{d}V/\mathrm{d}t), \qquad (1)$$

where $V(t)$ is the cell's action potential. Fig. 2 illustrates the separation of the capacitive from the ionic current. Fig. 2 *A* is the average of 15 sequential action potentials, and Fig. 2 *B* (trace *1*) is the average of 15 action currents each containing a component later identified as the Na current. Since every action current had active channels, it was impossible to use blank traces to subtract $i_c(t)$, as in a previous study (Mazzanti and DeFelice, 1987). Instead, we calculated $\mathrm{d}V/\mathrm{d}t$ from the average action potential and adjusted c until $c(\mathrm{d}V/\mathrm{d}t)$ matched the peak of the measured current. Fig. 2 *B* (trace *2*) is the derived current using $c = 0.5$ pF. Subtracting the two traces resulted in Fig. 2 *C*, which represents the average ionic current through the patch during the action potential.

This value of c contains not only the patch capacitance, c_p, but also a stray capacitance, c_s. The patch area implied by 0.5 pF is too large considering the tip diameter of the pipettes. To look for the source of the stray capacitance, we first recorded the action current with only the cell-attached electrode in place and then again with the voltage electrode in place. Fig. 3 *A* is a record of the action currents from the first electrode before (trace *1*) and after (trace *2*) placement of the second electrode. The channel activity and the amplitude of the inward ionic current is the same in both

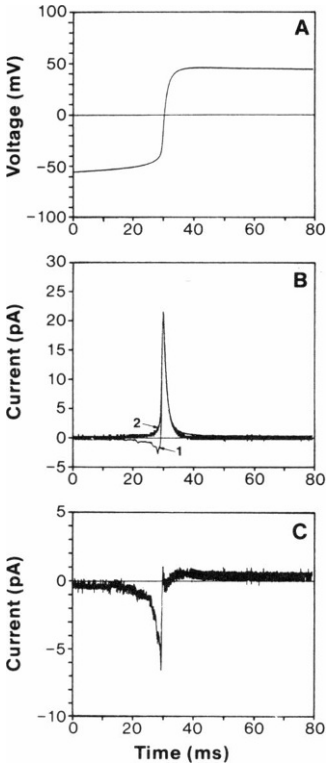

FIGURE 2 Subtracting the capacitive transient. (*A*) An action potential similar to that in Fig. 1 but on a faster time scale. (*B*) Trace *1* is an average of 15 action currents, each containing an inward ionic current; trace *2* is the scaled derivative, $c(\mathrm{d}V/\mathrm{d}t)$, of the action potential in *A*. (*C*) The result of subtracting the two traces in *B*.

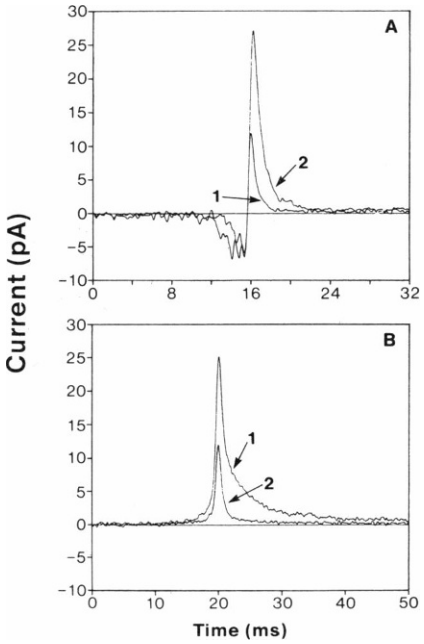

FIGURE 3 Measuring the coupling between the voltage and current electrodes. (*A*) A patch with ionic current. Trace *1* is an action current before placing the voltage electrode; trace *2* is an action current from the same patch after placing the voltage electrode. The ionic component of the action current (the inward current just before the outward capacitive transient) has the same amplitude with either one or two electrodes in place, but the capacitive current is roughly double in the two-electrode configuration. (*B*) A patch with no ionic current. Trace *1* is an action current recorded during a two-electrode experiment; trace *2* is from the same electrode after pulling it away from the cell and forming a vesicle in the tip. Thus, trace *2* in *B* represents the extraneous coupling factor between the current and voltage electrodes.

traces, not only for individual beats (shown in the figure), but also for the average over many beats (not shown). The capacitive transient, however, is at least doubled after placement of the second electrode, implying that the main source of the stray capacitance is the coupling between the cell-attached and whole-cell electrodes.

The measurement of c_p relies upon patches without channels but with similar capacitive current as patches with channels. After several beats, we pull the current electrode away to form a vesicle. The electrode's seal resistance remains the same, but its capacitive transient decreases by about half. Fig. 3 *B* (trace *1*) is the patch current, $i_c(t)$, with both electrodes in place; Fig. 3 *B* (trace *2*) is the patch current, $i_s(t)$, from the same electrode pulled away from the cell. The patch capacitance is then calculable from:

$$c_p = [i_c(t) - i_s(t)]/(dV/dt), \qquad (2)$$

where (dV/dt) comes from Fig. 4 *A*, and ["] is the corrected patch current in Fig. 4 *B*. Fig. 4 *C* plots this ratio. Assuming an ohmic leak with zero reversal potential, the leakage current through the patch is $gV(t)$. Calculating c_p when $V(t) = 0$ would eliminate such a term. An alternative voltage for assuming zero leakage might be the average value of V throughout the natural diastolic and systolic cycle, because ion concentrations tend to equilibrate on that value over long periods of time. The average value of V depends on the particular cell; it does indeed lie near the minimum of the curve in Fig. 4 *C*, rather close to $V = 0$. The value of c_p calculated anywhere along the flat portion of this curve will be fairly uniform: when $V = 0$, $c_p = 0.076$ pF. This method consistently gave values of $c_p < 0.1$ pF. Assuming 1 μF/cm^2, the upper limit for the area of a patch is 10 μm^2.

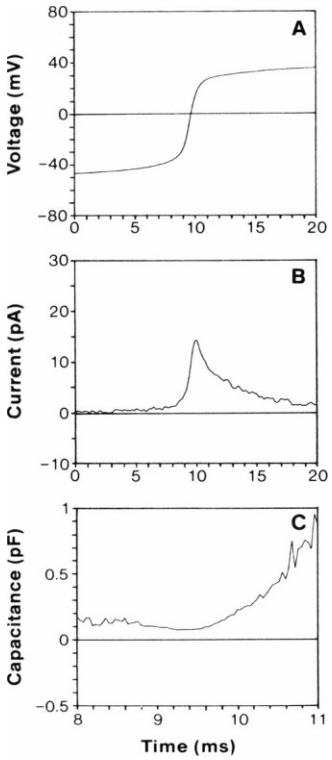

FIGURE 4 Measuring the patch area. (*A*) An action potential, $V(t)$, from the voltage electrode in a two-electrode experiment. (*B*) The simultaneous action current after subtracting the coupling factor (see Fig. 3). (*C*) The ratio of *B* and the time derivative of *A*, for a narrow range of time around the upstroke of the action potential.

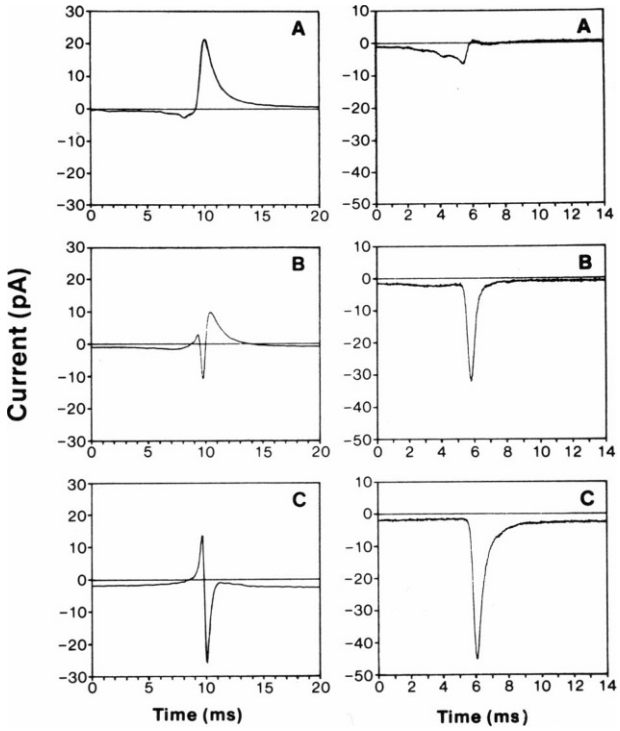

FIGURE 5 (*Left*): The effect of hyperpolarizing the patch. The action potential in this experiment is the same as that in Fig. 2 *A*. The action currents in *A*, *B*, and *C* are for pipette potentials V_p = 0, 20, and 40 mV, and they are average action currents over 15 consecutive beats. The action potential was identical for each V_p. (*Right*): The data on the left after subtracting the capacitive transient by the method of Fig. 2.

Identification of the Na Current

The experiment in Fig. 5 is the same as in Fig. 2, but it applies three pipette potentials: 0, 20, and 40 mV. Each panel in the left column is the average of 15 beats at the given potential. Using the method of Fig. 2, we subtract the capacitive current for each trace and plot the differences in the right column. Plotting the current in each frame against its corresponding voltage, $V(t) - V_p$, gave a reversal potential for the Na action current of $E = 30$ mV (Fig. 6). This protocol requires two-electrode experiments to ensure that, except for the negative offset, the action potentials remain identical for different V_ps.

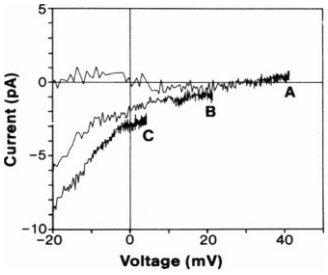

FIGURE 6 The reversal potential (*E*). Plotting the average ionic action currents in Fig. 5 (*right*) against their respective action potentials, $V(t) - V_p$, estimates the reversal potential for the inward current. At V_p = 0 mV, E = 30 mV; the experiments at V_p = 20 and 40 mV extrapolate to the same value.

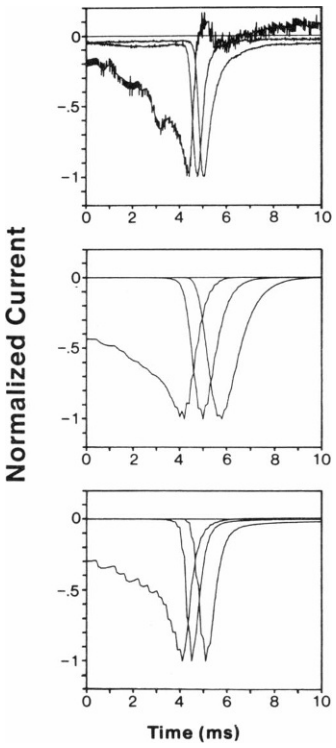

FIGURE 7 Comparing the Na current to models. (*A*) The three traces in *A* are normalized action currents from *A*, *B*, and *C* of Fig. 5 (*right*). *B* is a computer simulation using the Ebihara and Johnson (1980) model, and *C* is a computer simulation using the Hodgkin and Huxley (1952) model. We modified both models to our experimental conditions (Table I) and drove the models with the recorded action potential from the experiment of panel *A*. (See DeFelice et al., 1985).

Fig. 7 *A* shows the normalized experimental traces, and Figs. 7 *B* and 7 *C* are calculations from two models. In making the calculations, we used the measured action potential of Fig. 7 *A* to drive the models. Fig. 7 *B* is from Ebihara and Johnson (1980). (Instead of using the discontinuous functions for α_h and β_h that appeared in the original EJ model, we matched smooth functions to their data.) Fig. 7 *C* is from Hodgkin and Huxley (1952). In both cases, we used γ_{Na} = 15 pS, E_{Na} = 30 mV, and T = 24°; the single-channel conductance came from Cachelin et al. (1983), and E and T corresponded to our experimental conditions. Table I gives the actual rate constants that entered into the calculations.

Table II summarizes the EJ and HH models applied to our experiments. In the data column are peak Na currents at various V_ps. Forcing the models to match these amplitudes gave us the number of channels (N) in the patch. For example, to obtain −32 pA at V_p = 20 mV required 690 HH Na channels in the patch. A correct model should give a constant number at all potentials; of those we tried, only the HH equations reproduced the data at each potential using approximately the same N. Of the cardiac models, only Ebihara and Johnson's was able to generate the slow rising phase of the Na current at the foot of the action potential, but it gave too wide a range of N for different V_p and too large a value of N for V_p = 0 to be acceptable (see Discussion for more detail).

TABLE II
COMPARISON OF THE MEASURED Na CURRENT WITH TWO MODELS (SEE FIG. 8)

V_p	Peak current	N(EJ)	N(HH)
	pA		
0	−6.55	2,370	590
20	−32.1	200	690
40	−45.2	160	860

V_p is the voltage in the pipette. The peak Na current at each V_p appears in the second column, and the number of channels in the patch necessary to generate that current in two models appears in the last two columns.

Although most patches contained Na channels, some contained so few that none opened during an action potential. Since hyperpolarizing the patch increased the probability that channels opened, we compared patches with low and high densities by selecting a standard hyperpolarization of 20 mV and ranking the current in different patches. Matching the peak Na currents to the HH model in 15 experiments, we found patches that contained as few as 54 and as many as 690 channels. Using the maximum value of 10 μm^2 per patch, the minimum average density of Na channels in 7-d chick ventricle was 23/μm^2, with a standard deviation of ±21.

DISCUSSION

Fozzard and Sheu (1980), using ion-selective electrodes, measured 13 mM free, intracellular Na concentration in

TABLE I
A COMPARISON OF THE RATE CONSTANTS IN TWO MODELS OF THE NA CHANNEL AT T = 24°C

Ebihara-Johnson		Hodgkin-Huxley	
α_m: C_3 = 47.13	β_m: C_1 = 0.0205	α_m: C_3 = 35	β_m: C_1 = 21.6
C_4 = −0.082	C_2 = −0.0909	C_4 = −0.54	C_2 = −0.0556
C_5 = 47.13		C_5 = 35	C_3 = 60
C_6 = −0.1		C_6 = −0.1	
C_7 = −1		C_7 = −1	
α_h: C_1 = 0.0346	β_h: C_1 = 0.5078	α_h: C_1 = 0.378	β_h: C_1 = 5.4
C_2 = −0.147	C_3 = 25.475	C_2 = −0.05	C_3 = 30
C_3 = 80	C_6 = −0.09227	C_3 = 60	C_6 = −0.1
	C_7 = 0.2563		C_7 = 1

Rate = $\{C_1 \exp[C_2(V + C_3)] + C_4(V + C_5)\}/\{\exp[C_6(V + C_3)] + C_7\}$

embryonic chick ventricle. Since our patch pipette contained 130 mM Na, the expected reversal potential, assuming perfect selectivity, is 58 mV. A reversal potential of 30 mV, which we measure in the present study, implies an internal Na concentration of nearly 40 mM, three times higher than the free Na and more than the total average Na inside these cells (McDonald and DeHaan, 1973; flame photometry). Furthermore, the dynamic reversal potential of 30 mV remained the same whether or not a whole-cell electrode containing no Na was present. Both of these observations point to the conclusion that the beating heart cell determines the high Na concentration near the mouths of channels, and that the Na concentration near the membrane is independent of the bulk concentration. This reasoning is consistent with a previous result for Na-conducting Ca channels, which reversed at 25 mV in beating cells, but at 50 mV in nonbeating cells (Mazzanti and DeFelice, 1987).

A remarkable feature of our results is that the Hodgkin and Huxley model for the Na current works better than the standard models designed specifically for heart. The Ebihara and Johnson equations, for example, which describe step-protocol experiments on the very tissue we are studying, are less suitable for explaining action currents in patches than the classical HH equations. To understand how this comes about, notice that while both schemes use m^3h kinetics, EJ's model, like virtually all cardiac models, employs rate constants that are much lower than HH's when standardized to the same temperature. Two consequences of the lower rate constants are (*a*) EJ kinetics are fundamentally slower than HH's, and (*b*) EJ's h-infinity curve lies considerably to the left of HH's on the negative voltage axis. Although neither model fits perfectly, the quicker HH kinetics fit the patch currents better. Furthermore, the strong inactivation of the cardiac model during diastolic depolarization increases the number of Na channels cardiac models needed to reconstruct the current.

A larger or smaller number of channels would not in itself make one model preferable to another. However, hyperpolarizing a patch by 20 mV caused the required number of EJ channels to decrease by a factor of 10, whereas HH changed by only 20%. Since the total number of channels should be independent of voltage, the consistency of the HH model, plus its closer representation of the kinetics, led us to assume it, rather than the EJ model, to describe our experiments. The average channel density under HH kinetics is 23 Na channels/μm^2; EJ kinetics give four times this number. The lower amount is more reasonable, as we shall see below. This discrepancy vanishes if we consider the original step-protocol experiments to which the EJ equations actually apply: stepping from negative holding potentials, Ebihara and Johnson measured a $\bar{g}_{Na}$ of 23 mS/cm^2, or roughly 15 Na channels/μm^2. To further check these calculations, we derived the density from whole-cell data taken from Fujii et al. (1987): by fitting their currents to the HH model, we calculated an Na channel density of 17/μm^2, comparable to the average patch density of 23/μm^2 obtained from action currents.

To compare this density with densities in other cardiac tissues, note that Cachelin et al. (1982) found that Na channels in neonatal rat heart under physiological conditions had a conductance of 15 pS, similar to the value in nerve and muscle cells. (For the same tissue under slightly different conditions, Kunze et al. [1984] found a conductance of 20 pS.) Using 15 pS, the equivalent channel density from $\bar{g}_{Na}$ is 10/μm^2 for Purkinje fibers (McAllister et al., 1975) and 2.7/μm^2 for adult ventricle (Beeler and Reuter, 1977). A single-channel study by Brown et al. (1981) on adult rat heart resulted in 16/μm^2, and the two neonatal rat heart experiments quoted above gave between 1 and 2 Na channels per μm^2.

In conclusion, though 7-d chick ventricle cells have a total of over 17,000 Na channels on a surface membrane of 750 μm^2, the channel density varies between 5 and 70 per μm^2 in different regions. When the cell beats, Na concentration near the channel is nearly 40 mM, much higher than in the cytosol and high enough to support an outward current during an action potential. In beating cells, $< 10\%$ of the Na channels are open at any time and $< 2\%$ are open at the peak of the action current. The maximum Na current is roughly -300 pA/cell, an average of one open channel per 2 μm^2. If the Na current exactly matched the capacitive transient, 300 pA would imply a maximum upstroke velocity of 40 V/s, but the Na current is smaller and has a different shape, indicating the presence of other channels. A cell can generate larger currents by stepping from negative potentials. Such experiments measure channel densities that are consistent with the present study, but the kinetics they support do not describe the Na current that occurs naturally during the spontaneous beat of heart cells.

We thank Ms. B. Duke Cuti, Mr. W. N. Goolsby, and Ms. Elise Boswell for technical assistance. Special thanks go to Dr. Sally Wolff for her editorial comments on the manuscript.

National Institutes of Health grant HL-27385 supports this work.

Received for publication 21 November 1986 and in final form 20 March 1987.

REFERENCES

Beeler, G. W., and H. Reuter. 1977. Reconstruction of the action potential of ventricular myocardial fibres. *J. Physiol. (Lond.).* 286:177–210.

Bodewei, R., S. Hering, B. Lenke, L. V. Rosenhstraukn, A. I. Undrovings, and A. Wollenberger. 1982. Characterization of fast sodium current in isolated rat myocardial cells: simulation of the clamped membrane potential. *J. Physiol. (Lond.).* 325:301–315.

Brown, A. M., K. S. Lee, and T. Powell. 1981. Sodium current in single rat heart muscle cells. *J. Physiol. (Lond.).* 318:479–500.

Cachelin, A. B., J. E. dePeyer, S. Kokubun, and H. Reuter. 1983. Sodium channels in cultured cardiac cells. *J. Physiol. (Lond.).* 340:389–401.

DeFelice, L. J., W. Goolsby, and D. Huang. 1985. Membrane noise and excitability. *In* Noise in Physical Systems and 1/f Noise. A. D'Amico

and P. Mazzetti, editors. Elsevier Science Publishing Co. Inc., New York. 25–45.

DeHaan, R. L. 1967. Regulation of spontaneous activity and growth of embryonic chick heart cells in culture. *Dev. Biol.* 16:216–249.

DiFrancesco, D., and D. Noble. 1985. A model of cardiac electrical activity incorporating ionic pumps and concentration charges. *J. Physiol. (Lond.).* 307:353–398.

Ebihara, L., and E. A. Johnson. 1980. Fast sodium current in cardiac muscle. A quantitative description. *Biophys. J.* 32:779–790.

Fischmeister, R., L. J. DeFelice, R. K. Ayer, Jr., R. Levi, and R. L. DeHaan. 1984. Channel currents in embryonic chick heart cells. *Biophys. J.* 46:267–272.

Fozzard, H. A., and S. S. Sheu. 1980. Intracellular potassium and sodium activities of chick ventricular muscle during embryonic development. *J. Physiol. (Lond.).* 306:579–586.

Fujii, S., R. K. Ayer, and R. L. DeHaan. 1986. Differentiation of transmembrane ionic currents in the early embryonic chick heart. *In* Progress in Developmental Biology, Part A. H. C. Slavkin, editor Alan R. Liss Inc., New York. 353–356.

Hodgkin, A. L., and A. F. Huxley. 1952. A qualitative description of membrane current and its application to conduction and excitation in nerve. *J. Physiol. (Lond.).* 117:500–544.

Kunze, D. L., A. E. Lacerda, D. L. Wilson, and A. M. Brown. 1985. Single sodium channels in rat ventricular cells. *J. Gen. Physiol.* 86:691–719.

Lee, K. S., J. R. Hume, W. Giles, and A. M. Brown. 1981. Sodium current depression by lidocaine and quinidine in isolated ventricular cells. *Nature (Lond.).* 291:325–327.

Lee, K. S., T. A. Weeks, R. H. Kao, N. Akaike, and A. M. Brown. 1979. Sodium current in single heart muscle cells. *Nature (Lond.).* 278:269–271.

Levi, R., and L. J. DeFelice. 1986. Sodium-conducting channels in cardiac membranes in low sodium. *Biophys. J.* 50:5–9.

Mazzanti, M., and L. J. DeFelice. 1987. Regulation of the Na-conducting Ca channel during the cardiac action potential. *Biophys. J.* 51:115–121.

McAllister, R. E., D. Noble, and R. W. Tsien. 1975. Reconstruction of the electrical activity of cardiac Purkinje fibres. *J. Physiol. (Lond.).* 251:1–59.

McDonald, T. F., and R. L. DeHaan. 1973. Low levels and membrane potential in chick heart tissue and cultured cells. *J. Gen. Physiol.* 61:89–109.

Shrier, A., and J. Clay. 1986. Repolarization currents in embryonic chick atrial heart cell aggregates. *Biophys. J.* 50:861–874.